



HAL
open science

Automated markerless registration of point clouds from TLS and structured light scanner for heritage documentation

Jie Shao, Wuming Zhang, Nicolas Mellado, Pierre Grussenmeyer, Renju Li,
Yiming Chen, Peng Wan, Xintong Zhang, Shangshu Cai

► **To cite this version:**

Jie Shao, Wuming Zhang, Nicolas Mellado, Pierre Grussenmeyer, Renju Li, et al.. Automated markerless registration of point clouds from TLS and structured light scanner for heritage documentation. *Journal of Cultural Heritage*, 2018, 32, pp.16-24. 10.1016/j.culher.2018.07.013 . hal-01884798

HAL Id: hal-01884798

<https://hal.science/hal-01884798>

Submitted on 19 Nov 2019

HAL is a multi-disciplinary open access archive for the deposit and dissemination of scientific research documents, whether they are published or not. The documents may come from teaching and research institutions in France or abroad, or from public or private research centers.

L'archive ouverte pluridisciplinaire **HAL**, est destinée au dépôt et à la diffusion de documents scientifiques de niveau recherche, publiés ou non, émanant des établissements d'enseignement et de recherche français ou étrangers, des laboratoires publics ou privés.

Automated Markerless Registration of Point Clouds from TLS and Structured Light Scanner for Heritage Documentation

Jie Shao ^{a,b,c}, Wuming Zhang ^{b,*}, Nicolas Mellado ^c, Pierre Grussenmeyer ^d, Renju Li ^e,
Yiming Chen ^b, Peng Wan ^b, Xintong Zhang ^b, Shangshu Cai ^b

^a Beijing Advanced Innovation Center for Imaging Technology, Capital Normal University, Beijing 100048, China

^b State Key Laboratory of Remote Sensing Science, Institute of Remote Sensing Science and Engineering, Faculty of Geographical Science, Beijing Normal University, Beijing 100875, China

^c IRIT, CNRS, University of Toulouse, Toulouse 31062, France

^d ICube Laboratory, Photogrammetry and Geomatics Group, National Institute of Applied Sciences (INSA), Strasbourg 67084, France

^e Beijing TenYoun 3D Technology Co., Ltd., Beijing 100083, China

ABSTRACT

Three-dimensional (3D) model is a major form of cultural heritage documentation. In most cases, the properties of digital artefacts (e.g. readability, coverage) are affected by the acquisition procedure (e.g. device, workflow, conditions) and the characteristics of the physical artefact (e.g. shape, size and materials). In this paper, we study how to combine two acquisition techniques to acquire detailed 3D models of large physical objects. Specifically, we combine two laser scanning instruments: Terrestrial Laser Scanning (TLS) and Structured Light Scanner (SLS). TLS provides millimeter-scale resolution with large field of view, while SLS provides sub-millimeter resolution for limited field of view. This paper focuses on the registration of SLS and TLS point clouds, a critical step which aims at aligning the acquired point clouds in a common frame. Existing registration systems mostly rely on manual post-processing or marker-based alignment. Manual registration is however time consuming and tedious, while markers increase the complexity of scanning and are not always acceptable in cultural site documentation. Therefore, we propose an automated markerless registration and fusion pipeline for point clouds. Firstly, we replace the marker-based coarse alignment by an automated registration of SLS and TLS point clouds; secondly, we refine the alignment of SLS point clouds on TLS data using the Iterative Corresponding Point algorithm; finally, we seamlessly stitch the SLS and TLS point clouds by globally regularizing the registration error for all the point clouds at once. Our experiments show the efficiency of the proposed approach on two real-world cases, involving detailed point clouds correctly aligned without requiring markers or manual tuning. This paper provides an operational process reference for automated markerless registration of multi-source point clouds.

Keywords: heritage documentation; terrestrial LiDAR; structured light scanner; point clouds registration

1 Introduction

The digitalization of Cultural Heritage material is nowadays a common process, enabling long term archiving, simple sharing and digital presentation for research and diffusion to the general public [1]. Due to the rich information usually found in Cultural Heritage materials, e.g. fine and vivid work art, complex and diverse surface, 3D digitalization is today becoming the standard in most application cases, yielding important research efforts for the 3D modeling of Cultural Heritage content. Especially, the choice of a specific acquisition technique is a determining factor for the quality and properties of the virtual description of the Cultural Heritage artefacts. In some cases, it might be necessary to combine multiple acquisition techniques at once [2], which imply a final registration step to merge the heterogeneous data in a unique and consistent

* Corresponding author.

E-mail address: wumingz@bnu.edu.cn (Wuming Zhang).

38 model.

39 The simplest form of 3D models is a set of 3D coordinates sampling an object surface, called a point cloud.
40 Most acquisition techniques acquire physical objects as point clouds, e.g., laser scanners, structure from motion
41 and structured light [3]. Laser scanning is nowadays a very common acquisition technique, and we refer the
42 interested reader to the survey by Vacca et al. [4] on laser-based acquisition for Cultural Heritage applications.
43 We consider in this work Terrestrial Laser Scanning (TLS). A TLS instruments can provide high precision 3D
44 point cloud with millimeter accuracy over varying field of views. In practice, devices with large field of view
45 (e.g., 360 degrees in the horizontal direction) have low horizontal sampling rate which reduces the amount of
46 details acquired by the scanner. Structure from motion (SFM) extracts corresponding points from overlapping
47 images and generates detailed 3D models [5], but without guaranteed accuracy and correctness [6]. Meanwhile,
48 in some specific cases with high surface erosion and other defects, the lack of texture information might limit
49 the efficiency of SFM techniques. Instead of relying on the surfaces textures, Structured Light Scanners (SLS)
50 project light patterns on the object and obtains a point cloud model from distortions of the pattern [7-8],
51 reaching submillimeter accuracy [9]. Compared with TLS, SLS can get more detailed 3D point clouds.
52 However, due to their limited field of view, SLS instrument might require multi-station scanning to acquire
53 large-scale objects or scenes.

54 This motivates the need of 3D registration techniques, which align several point clouds acquired from
55 different points of view and/or with different instruments. Marker-based registration requires positioning
56 artificial markers in scene, and then using these markers to find correspondences between several scans and
57 align the associated point clouds [10]. In practice, complex scenes might require to set a large number of
58 markers so they are visible in multiple scans. In addition to be time consuming, fixing markers on ancient
59 objects might cause secondary damage to the cultural heritage site, which is obviously undesirable. Instead of
60 using physical markers, several techniques automatically extract geometric features, assuming they will be
61 detected consistently in the input point clouds and used as marker substitutes by the registration algorithms
62 [11-12]. In practice however, descriptor-based approaches might not be robust to variations of noise, details
63 and missing data, i.e. the defects that are usually occurring when processing point clouds generated by multiple
64 acquisition systems [13]. Alternatively, exploration-based registration approaches explore the space of rigid
65 transformations to find the configuration maximizing a given metric (e.g., overlap). The state-of-the-art
66 algorithm is 4-Points Congruent Sets (4PCS) [14-15], which matches almost-planar 4-point basis in two input
67 clouds. Despite its efficiency, this approach might in some cases require a lot of computational time [16]. More
68 recently, the variant Super4PCS [17] greatly increased the computational efficiency of 4PCS by reducing the
69 computational complexity required for the exploration.

70 We also refer the interested reader to the survey by Gomes et al [18], where the authors review the principal
71 steps and associated challenges related to the acquisition and processing of 3D content for Cultural Heritage
72 documentation. After acquisition and coarse registration, the 3D point clouds transformations need to be
73 refined to avoid error accumulation occurring when combining multiple pairwise registrations.

74 **2 Research aim**

75 In order to obtain robust, accurate and detailed 3D models of cultural heritage sites in a non-destructive way,
76 this work combine the advantages of TLS (e.g., large-scale) and SLS (e.g., accuracy) for 3D modeling of
77 Longmen Grottoes. A TLS point cloud represents the whole cultural heritage site, and each SLS point cloud is
78 a detailed part of it. These point clouds are aligned automatically by Super4PCS, and then pairwise registration
79 and global regularization are applied to the point clouds to generate the final 3D models. The main
80 contributions of this work is a practical system for the automated registration of multiple point clouds with

81 varying accuracy and sampling, allowing large scale acquisition of Cultural Heritage sites with locally detailed
82 areas.

83 The rest of this paper is structured as follows: Section 3 describes the experimental material and the
84 registration method of point clouds. The experimental results are presented and discussed in Section 4. Finally,
85 the conclusions are stated in Section 5.

86 **3 Material and methods**

87 *3.1 Data description*

88 Excavation of Longmen Grottoes (Fig. 1) has been ongoing since 493 AD. It is one of three notable stone
89 carving treasures in China and is known as one of the world's greatest classical art treasures. The site was
90 placed upon the UNESCO World Heritage List in 2000, and the World Heritage Committee evaluated that
91 Longmen Grottoes and Buddha is the largest and the most outstanding plastic arts from the later period of
92 Northern Wei Dynasty to the Tang dynasty. These art pieces, which describe religious subjects of Buddhism
93 in detail, represent the peak of Chinese art [19]. The protection of Longmen Grottoes has great significance for
94 Chinese civilization and human art, and motivates its documentation and archiving.

95 In the past, manual measurement was the main way of cultural heritage information acquisition. In recent
96 years, with the development of computer technology, photogrammetry, LiDAR, computer graphics and so on,
97 protection of cultural heritage has progressed speedily, and displayed in the form of 3D model. 3D model has
98 been widely applied in cultural heritage sites of the world by rich spatial information and the development of
99 3D information acquisition sensors [20-21]. However, because of long-term sunlight exposure, rain erosion
100 and weathering factors, Longmen Grottoes statues have become so fragile that collapses occurred at any time.
101 Therefore, high accuracy and non-destructive acquisition of 3D models is urgent for protection of Longmen
102 Grottoes at present. Due to the fine and detailed structure information of Longmen Grottoes, the resolution of
103 TLS is not enough to meet the demand; SLS has a higher resolution, but its field of view is limited, and multiple
104 SLS point clouds registration easily produces cumulative error. Therefore, this paper combined the advantages
105 of SLS and TLS to obtain 3D surface information of Longmen Grottoes statue.

106 The device parameters of SLS and TLS are shown in Table 1. For our experiments, we focused on one statue
107 as experimental sample, and the height of the statue is nearly 0.6 m, the average width of the statue is nearly
108 0.3 m. 1 TLS point cloud and some SLS point clouds are acquired as follows (Fig. 2).

109 *3.2 Method*

110 In order to perform automated markerless registration of point clouds from TLS and SLS for heritage
111 documentation, this paper studies the registration from three aspects: pairwise coarse and fine registration, and
112 global regularization. Coarse registration processes pairs of point clouds to align them roughly; fine registration
113 refines the rough transformation estimate; global regularization removes the cumulative error introduced when
114 combining multiple pairwise registrations. The workflow is as shown in Fig. 3.

115 *3.2.1 Coarse Pairwise Registration*

116 The goal of the coarse pairwise registration step is to find the relative position of each SLS point cloud on
117 the TLS point cloud. As previously stated, marker-based alignment can provide such rough estimate, however
118 it increases the acquisition time and may damage the cultural heritage artefacts. Alternatively, we propose in
119 this work to use the state of the art registration technique Super4PCS, an algorithm which computes the rough
120 alignment between one *source* point cloud to a *target* point cloud. In order to align all SLS point clouds on the
121 same reference frame, we sequentially register each SLS point clouds on the TLS point cloud.

122 Super4PCS estimates a coarse alignment between two point clouds by exploring the set of rigid
123 transformations (rotations and translations) using the input point clouds as priors. More formally, it selects 4
124 almost coplanar points in the *target* point cloud to form a so-called 4-point basis. Then it looks for all 4-points
125 configurations with similar geometric properties in the *source* point cloud. For each configuration, a geometric
126 transformation candidate T_i is computed by aligning the 4-points to the basis in the *target* cloud. Super4PCS
127 selects the transformation that maximizes the overlap between the *source* and *target* clouds. The input point
128 clouds are locally overlapping if their distance is locally less than a given threshold. Considering that the TLS
129 point cloud has been acquired with 5 millimeters precision, we set the overlapping distance threshold at 1
130 centimeter for all our experiments. We used the implementation provided by the OpenGR library [22] for our
131 experiments (Fig. 4 (a)).

132 Fig. 4 (a) shows two results of coarse alignment between a SLS point cloud (white) and the TLS point cloud
133 (red). Super4PCS outputs correct rough estimate of the transformations, i.e. the SLS point clouds are overall
134 well positioned on the TLS point cloud, but still need to be further refined in a second step.

135 3.2.2 Fine Pairwise Registration

136 The goal of the fine pairwise registration step is to slightly move the SLS point clouds so they fit as much
137 as possible the TLS point cloud. This is a very standard process in point cloud processing, also known as local
138 pairwise registration. The reference algorithm to solve this problem is the Iterative Closest Point (ICP)
139 algorithm that was proposed by Besl and Mckay [23]. ICP is an iterative algorithm that minimizes the distance
140 between pairs or corresponding points in the two point clouds. The algorithm repeats the selection of
141 corresponding points to compute an optimal rigid-body transformation until converging on accurate matching
142 results. Several variants have been proposed under the name Iterative Corresponding Point (see recent survey
143 by Pomerleau et al. [24]), and ICP is nowadays considered as a very mature algorithm, implemented in most
144 3D software.

145 In a nutshell, given a *source* point cloud (in our case, any SLS cloud) and a *target* point cloud (in our case,
146 the TLS cloud), the ICP algorithm first establishes a set of pair-correspondences between points in two clouds.
147 Then, it computes a 3D rigid-body transformation minimizing a given error metric between the corresponding
148 points, e.g. the point-to-plane distance.

149 To be consistent with the parameters used during the coarse registration step, we set the ICP error threshold
150 at 1cm, the maximum number of iteration to 20, and the convergence threshold $\eta = 1.0^{-5}$. We show in Fig.
151 4 (b) how ICP refines the transformations (we used CloudCompare [25] for our experiments).

152 In this example, ICP produces good results even if it has to solve a relatively large motion between the rough
153 estimate and the target configuration (Fig. 4 (b)). As registration is performed only between each SLS point
154 cloud and the TLS point cloud, there is no guaranty that two overlapping SLS point cloud will be well aligned
155 by this process (in blue boxes of Fig.4 (b)). This motivates the need of final global regularization to minimize
156 the registration error globally between all point clouds.

157 3.2.3 Global regularization

158 In order to ensure gapless registration, we propose to globally adjust the sequence of SLS point clouds and
159 TLS point cloud with a large overlap. As some point clouds may overlap, and other not, we propose to build a
160 pose graph (Fig. 5) as follow: each point cloud is a vertex in the graph (denoted $TLSv_0$ or $SLSv_i$), and two
161 vertices are connected by an edge e_i if the associated point clouds are overlapping. As for previous stages, we
162 consider that two clouds are overlapping if their local distance is less than 1 centimeter, and we request at least
163 30% overlap to create an edge. As the SLS point clouds have been registered to the *source* TLS point cloud in
164 previous steps, it is very likely that all SLS v_i vertices are connected to $TLSv_0$ in the graph.

165 Once the graph is created, we use multi-view ICP [26], an extension of the ICP algorithm that minimizes
166 the registration error between multiple point clouds at once. It follows the overall ICP algorithm, except that
167 the error is computed for all pairs of points between all connected clouds. It outputs the set of transformations
168 for all the movable vertices in the pose graph. In our case, all SLS vertices v_i are marked as movable, but not
169 the TLS_{v_0} , which defined the common registration basis for the whole dataset. We used the implementation
170 by Glira et al [27], and use same stopping criterions as for fine pairwise registration. The result of global
171 regularization is shown as Fig. 6.

172 4 Results and discussion

173 We evaluated our approach on two datasets, acquired on two different Buddha in Longmen Grottoes (see
174 statistics in Table 2). Each dataset is composed by one reference TLS point cloud spanning the whole scene,
175 and multiple SLS point clouds detailing parts of the scene. The variations of sampling and amount of details
176 between the SLS and TLS point clouds are shown in Fig. 7.

177 In this section, we evaluate each step of our approach on scene 2 that we believe challenging, considering:

- 178 1) The symmetry of the scene, which may introduce ambiguities at the coarse registration step,
- 179 2) The large feature-less regions that prevent to use descriptor-based alignment, and,
- 180 3) The variation of sampling and level of details between the SLS and TLS point clouds.

181 We also demonstrate in supplementary materials how our approach performs on scene 2. All our experiments
182 have been performed on an Intel Xeon E5-2640 2.40GHz with 40 cores. We emphasize that both the coarse and
183 fine registration steps can be ran in parallel, in order to align each SLS point cloud to the TLS reference point
184 cloud simultaneously. We used single thread Matlab implementation [29] for our experiments, and better
185 performances can be expected with optimized code. For our experiments we stop the ICP iterations when the
186 registration error increases. As shown in Table 2, computing the coarse alignment between all clouds in parallel
187 takes 2m15s with our setup, for 91m30s of total processing time. In addition, TLS point cloud and all SLS
188 point clouds of all scenes were re-sampled according to the voxel size of 1 mm for the global regularization.

189 4.1 Coarse and fine pairwise registration

190 To evaluate the robustness of the coarse registration step, we used a fixed set of parameters for the whole
191 dataset: target overlap 90%, registration tolerance 5mm, and 2500 samples per point cloud. Registration results
192 are shown in Fig. 8. 39 SLS point clouds were correctly registered (in white, Fig. 8(a)), and 2 SLS point clouds
193 were not correctly registered (in yellow, Fig. 8(b-c)).

194 As shown in Fig. 8(c), the two SLS point clouds describe mostly flat surfaces with low but regular curvature.
195 The Super4PCS algorithm finds the transformation that maximizes the overlap between the two input clouds
196 given the input tolerance value. In these two cases, it appears that this metric is not enough to distinguish
197 between the correct pose and the found pose, where the SLS point cloud spans a part of the TLS point cloud.
198 In practice, these two failure cases might be corrected by adjusting the Super4PCS parameters; we obtained
199 good results by reducing the target overlap to 80%.

200 In summary, except for two features-less point clouds, all of the SLS point clouds can be registered with the
201 TLS point cloud, which shows the high reliability of the Super4PCS algorithm for coarse registration. Also, in
202 all cases we could refine the estimated transformation using ICP (see Section 3.2.2).

203 4.2 Global regularization

204 During the coarse alignment and fine registration steps, each SLS point cloud is registered to the reference
205 TLS point cloud, without considering the registration error between adjacent SLS point clouds. In practice,

206 these gaps do not meet the standard of heritage documentation, and a global regularization is required.

207 In this section we evaluate the influence of the TLS point cloud in the global regularization step. In Fig. 9(a),
208 we show results of scene 1, where only SLS point clouds are considered in the global regularization graph. The
209 goal of this experiment is to simulate the registration of detailed point clouds without using a reference point
210 cloud. Unsurprisingly, the SLS point clouds are correctly aligned, but the surface they describe deviates from
211 the TLS point cloud: registration error is accumulated and the overall registration quality is reduced even if the
212 registration error remains low.

213 On the other hand, we show in Fig. 9 (b) how using the TLS point cloud as reference greatly improves the
214 registration result. By combining SLS-SLS and SLS-TLS registration at once, our approach provides point
215 clouds with low local and global registration error.

216 **5 Conclusions**

217 The paper researched an automated markerless registration of SLS point clouds and TLS point cloud for the
218 heritage documentation of Longmen Grottoes Buddha from three aspects: coarse alignment, pairwise
219 registration, and global regularization. Our experiments showed that the SLS clouds can represent accurate
220 surface information of Buddha, but may lead to high accumulative error due to the registration process. On the
221 other hand, the TLS could get a whole 3D model of Buddha with one scanning, but the surface information is
222 not detailed enough. The combination of SLS and TLS could not only represent details for the whole Buddha
223 site, but also remove the accumulative error of a sequence of SLS point clouds registration. Besides, automated
224 markerless registration approach reduced dependence on artificial markers and manual work, which improved
225 the work efficiency. The proposed method provides an operational pipeline reference for automated markerless
226 registration of multi-source point clouds. All our experiments were performed using available processing tools,
227 and we will provide macros and scripts as reference for workers of digital documentation of heritage and point
228 cloud processing.

229 The main aim of this research is to explore an automated markerless registration approach of point clouds
230 for heritage documentation. The first step of our pipeline, i.e., coarse alignment, is a key factor in automated
231 registration of point clouds. In case of feature less surfaces, it might however fail in some cases and becomes
232 the main limitation for the high success rate of registration. In future work, we will focus on reducing the
233 sensitivity of parameters which influence the success rate of coarse alignment and thus improving the success
234 rate of the overall pipeline.

235 **Acknowledgements**

236 This work was supported by the National Key Research and Development Program of China Grant No.
237 (NO.2016YFB0501404) and the National Natural Science Foundation of China Grant Nos. 41671414,
238 41331171 and 41171265. This work was also supported by the Open Research Fund of Key Laboratory of
239 Digital Earth Science, Institute of Remote Sensing and Digital Earth, Chinese Academy of Sciences Grant No.
240 2014LDE015.

241 **References**

- 242 [1] F. Remondino, A. Rizzi, Reality-based 3D documentation of natural and cultural heritage sites-techniques, problems, and
243 examples, *Applied Geomatics*, 2010, pp. 85-100.
- 244 [2] W. Zhang, C. Wang, X. Xi, 3D scan of ornamental column (huabiao) using terrestrial lidar and hand-held imager, *ISPRS*,
245 *International Archives of the photogrammetry, Remote Sensing and Spatial Information Sciences*, XL-5/W7(2015) 491-
246 494.

- 247 [3] C.G. Serna, R. Pillay, A. Trémeau, Data fusion of objects using techniques such as laser scanning, structured light and
248 photogrammetry for cultural heritage applications, *Lecture Notes in Computer Science - Computational Color Imaging*,
249 2015, pp. 208-224.
- 250 [4] G. Vacca, M. Deidda, A. Dessi, M. Marras, Laser scanner survey to cultural heritage conservation and restoration, *ISPRS*
251 *International Archives of the Photogrammetry, Remote Sensing and Spatial Information Sciences*, XXXIX-B5(2012) 589-
252 594.
- 253 [5] J. McCarthy, Multi-image photogrammetry as a practical tool for cultural heritage survey and community engagement. *J.*
254 *Archaeol. Sci.* 43(2014) 175-185.
- 255 [6] C. Santagati, L. Inzerillo, F.D. Paola, Image-based modeling techniques for architectural heritage 3d digitalization: limits
256 and potentialities, *The International Archives of the Photogrammetry, Remote Sensing and Spatial Information Sciences*,
257 Volume XL-5/W2(2013) 550-560.
- 258 [7] J.W., Liu, Z.Q. Jiang, X. Sun, H. Hu, Integration of close range photogrammetry and structured light scanner for cultural
259 heritage documentation, *Advanced Materials Research*, 2012, pp. 1966-1969.
- 260 [8] D. Akca, 3D modeling of cultural heritage objects with a structured light system, *Mediterranean Archaeology &*
261 *Archaeometry*, 12(2012) 139-152.
- 262 [9] F. Buchónmoragues, J.M. Bravo, M. Ferri, J.V. Sánchezpérez, Application of structured light system technique for
263 authentication of wooden panel paintings, *Sensors*. 16(2016) 881-890.
- 264 [10] T. Hilker, N.C. Coops, D.S. Culvenor, G. Newnham, M.A. Wulder, C.W. Bater, A. Siggins, A simple technique for co-
265 registration of terrestrial LiDAR observations for forestry applications, *Remote Sens. Lett.* 3(2012) 239-247.
- 266 [11] P.M. Segundo, L. Gomes, O.R.P. Bellon, L. Silva, Automating 3D reconstruction pipeline by surf-based alignment, *IEEE*
267 *International Conference on Image Processing*, 2012, pp. 1761-1764.
- 268 [12] G. Bitelli, G. Castellazzi, A.M. D'Altri, S.D. Miranda, A. Lambertini, I. Selvaggi, Automated voxel model from point clouds
269 for structural analysis of cultural heritage, *The International Archives of the Photogrammetry, Remote Sensing and Spatial*
270 *Information Sciences*, XLI-B5(2016) 191-197.
- 271 [13] N. Mellado, M. Dellepiane, R. Scopigno, Relative scale estimation and 3D registration of multi-modal geometry using
272 Growing Least Squares, *IEEE Transactions on Visualization and Computer Graphics*, 22(2016) 2160-2173.
- 273 [14] D. Aiger, N.J. Mitra, D. Cohen-Or, 4-points congruent sets for robust pairwise surface registration, *ACM Trans. Graph.*
274 27(2008) 1-10.
- 275 [15] P.W. Theiler, J.D. Wegner, K. Schindler, Markerless point cloud registration with keypoint-based 4-points congruent sets,
276 *ISPRS Annals of the Photogrammetry, Remote Sensing and Spatial Information Sciences*, Vol. II-5/W2(2013) 283-288.
- 277 [16] P.W. Theiler, J.D. Wegner, K. Schindler, Keypoint-based 4-points congruent sets - automated marker-less registration of
278 laser scans, *ISPRS-J. Photogramm. Remote Sens.* 96(2014) 149-163.
- 279 [17] N. Mellado, D. Aiger, N.J. Mitra, SUPER 4PCS fast global pointcloud registration via smart indexing, *Comput. Graph.*
280 *Forum*, 33(2014) 205-215.
- 281 [18] L. Gomes, O.R.P. Bellon, L. Silva, 3D reconstruction methods for digital preservation of cultural heritage: A survey, *Pattern*
282 *Recognit. Lett.* 50(2014) 3-14.
- 283 [19] D. Wang, Internationalizing heritage: UNESCO and China's Longmen Grottoes, *China Information*, 24(2010) 123-147.
- 284 [20] O. Chee, C. Siew, Z. Majid, H. Setan, 3D documentation and preservation of historical monument using terrestrial laser
285 scanning, *Geoinformation Science Journal*, 10(2010) 73-90.
- 286 [21] M.L. Brutto, M. Spera, Image-based and range-based 3d modelling of archaeological cultural heritage: the Telamon of
287 Temple of Olympian ZEUS in Agrigento (Italy), *ISPRS – International Archives of the Photogrammetry, Remote Sensing*
288 *and Spatial Information Sciences*, 16(2012) 515-522.
- 289 [22] OpenGR: A C++ library for 3D Global Registration, N. Mellado and others, Accessed May 2018.
- 290 [23] P.J. Besl, N.D. McKay, A method for registration of 3-D shapes, *IEEE T. Pattern Anal.* 14(1992) 239-256.

- 291 [24] F. Pomerleau, F. Colas, R. Siegwart, A Review of Point Cloud Registration Algorithms for Mobile Robotics. *Found. Trends*
292 *Robot*, 4(2015) 1-104.
- 293 [25] CloudCompare. 3D point cloud editing and processing software, 2015
294 (<http://www.cloudcompare.org/doc/wiki/index.php?title=ICP>. Accessed 6 October 2015).
- 295 [26] K. Pulli, Multiview registration for large data sets, In *Proceedings of the 2nd international conference on 3-D digital imaging*
296 *and modeling (3DIM'99)*, IEEE Computer Society, Washington, DC, USA, 1999, 160-168.
- 297 [27] P. Glira, N. Pfeifer, C. Ressel, C. Briese, A correspondence framework for ALS strip adjustments based on variants of the
298 ICP algorithm, *Journal for Photogrammetry, Remote Sensing and Geoinformation Science*, 2015, pp. 275-289.
- 299 [28] R. Vergne, R. Pacanowski, P. Barla, X. Granier, C. Schlick, Radiance Scaling for Versatile Surface Enhancement, *I3D 10:*
300 *Proc. symposium on Interactive 3D graphics and games*, Feb 2010, Boston, United States. ACM, 2010.
- 301 [29] GlobalICP Matlab scripts, Philipp Glira, Accessed May 2018.

302 **Figure captions**

303 **Fig.1.** Longmen Grottoes.

304 Longmen Grottoes is one of three notable stone carving treasures in China and is known as one of the world's greatest classical
305 art treasures. The World Heritage Committee evaluated that Longmen Grottoes and Buddha is the largest and the most
306 outstanding plastic arts from the later period of Northern Wei Dynasty to the Tang dynasty.

307 **Fig. 2.** Point cloud of Longmen Grottoes statue.

308 (a) shows two SLS point clouds of a statue; (b) shows one TLS point cloud of a statue.

309 **Fig. 3.** The registration pipeline and overview.

310 (a) shows the schematic view of the registration pipeline; (b) shows the overview of the registration pipeline from a data
311 perspective, which includes four steps: (1) input, (2) coarse registration, (3) fine registration, and (4) global registration. The
312 input consists of two types of point clouds: one sparse (TLS, in orange) and multiple dense (SLS). After fine registration between
313 each SLS point clouds and the TLS reference point clouds, misalignments between SLS point clouds (black circle in the figure
314 of fine registration) are solved by the process of global registration.

315 **Fig. 4.** Results of Super4PCS and fine pairwise registration.

316 (a) shows the result of Super4PCS, which estimates the transformation between each SLS point clouds (white) and the TLS point
317 cloud (red); (b) shows the result after fine pairwise registration, where the transformations are refined with ICP. Note that the
318 overlapping parts (blue box) may not be properly aligned as the error between the SLS point clouds is not considered for these
319 two steps.

320 **Fig. 5.** Pose graph of global regularization.

321 SLS point clouds $\{v_1, v_2, v_3 \dots v_n\}$ are overlapping with the TLS point cloud and thus connected to v_0 . Also, all pairs of SLS point
322 clouds with at least 30% overlap are connected in the graph.

323 **Fig. 6.** Global regularization results.

324 (a) shows the result of 16 SLS point clouds registration; (b) shows the TLS point cloud; (c) shows TLS and SLS point clouds in
325 the same frame.

326 **Fig. 7.** The variations of details between SLS and TLS point cloud.

327 SLS point cloud (a) and TLS point cloud (b) from scene 1 rendered with Radiance Scaling [28].

328 **Fig. 8.** Results of coarse alignment.

329 (a) shows correct coarse alignment between each SLS point cloud and TLS point cloud; (b) shows incorrect coarse alignment;
330 (c) shows the 2 incorrect SLS point clouds.

331 **Fig. 9.** Results of global regularization.

332 (a) shows the global regularization result of only SLS point clouds, (a-1) and (a-2) show the horizontal and vertical cross section
333 of point cloud in yellow box, respectively; (b) shows the global regularization result combining TLS with SLS point clouds, (b-
334 1) and (b-2) show the horizontal and vertical cross section of point cloud in yellow box, respectively. (TLS in red; SLS in white)

335 **Tables**

336 **Table 1**

337 Device parameters

Parameters	SLS	TLS
Model	OKIO-5M-400	RIEGL VZ-1000
Max measure distance	1.5 m	1,200 m
Field of view	0.4m × 0.3m (at max distance)	100° × 360°
Measure precision	0.015 mm	5 mm

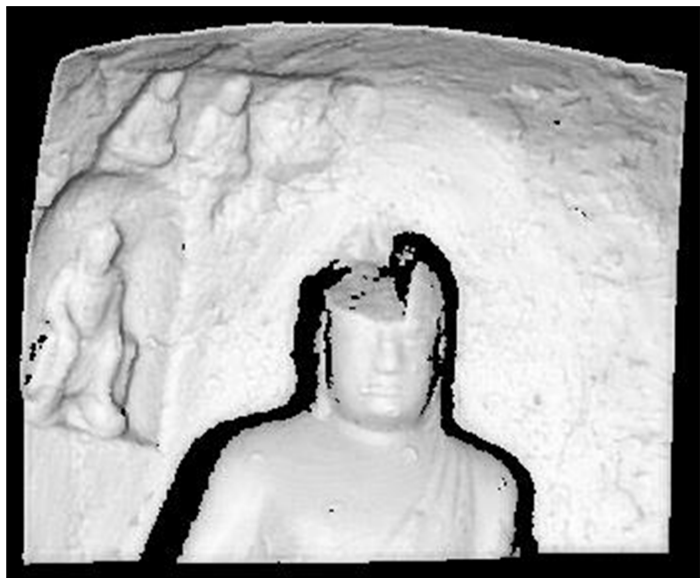
338 **Table 2**

339 Datasets properties and processing time. For the coarse alignment and fine registration steps, we detail for each scene the
 340 processing time needed to register the SLS point cloud on the TLS point cloud in parallel, and the total time when registering the
 341 SLS point clouds sequentially on a single processing unit.

	SLS point clouds		TLS point cloud	Processing time – pairwise (total)		
	#clouds	#vertices/cloud d	#vertices	Coarse registration	Fine registration	Global regularization
Scene 1	16	859,774	2,777,511	1m10s (18m40s)	3.1s (50s)	12.7m
Scene 2	41	926,830	2,732,000	2m15s (91m30s)	4.8s (3m20s)	27.5m

342

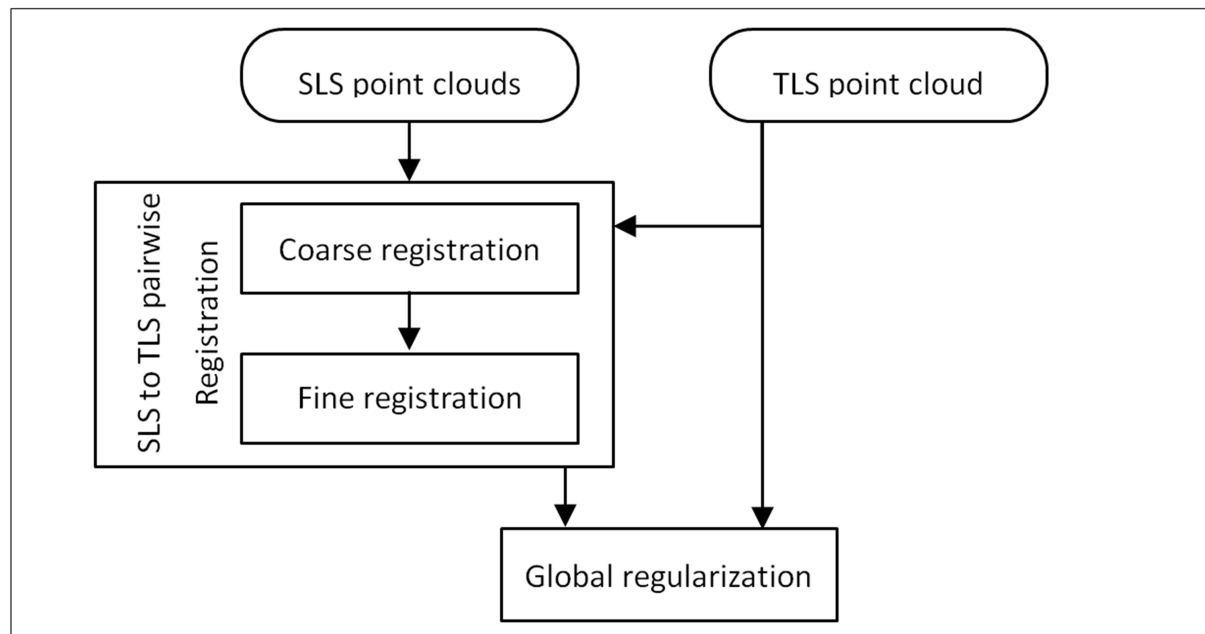




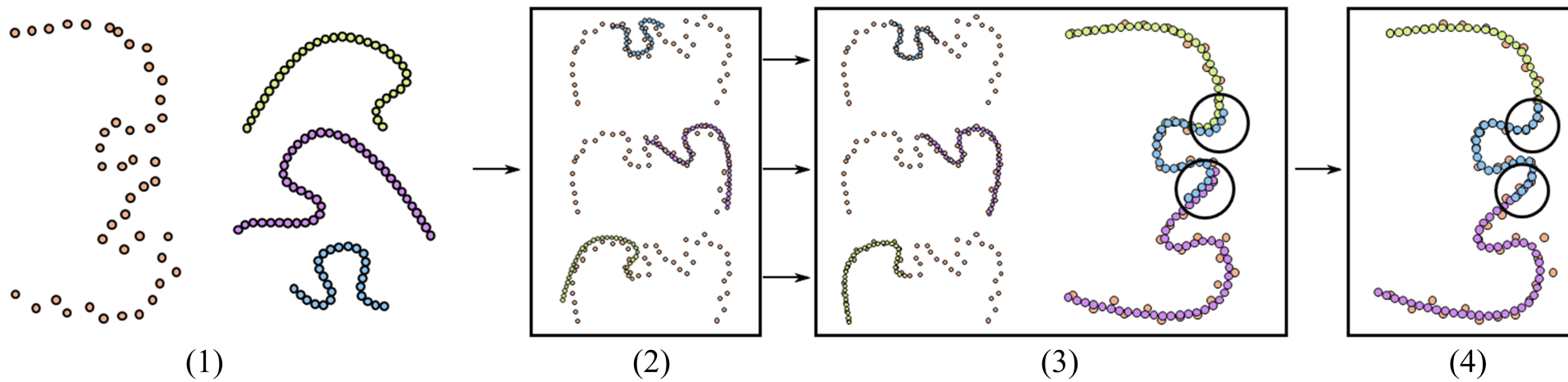
(a)



(b)



(a)



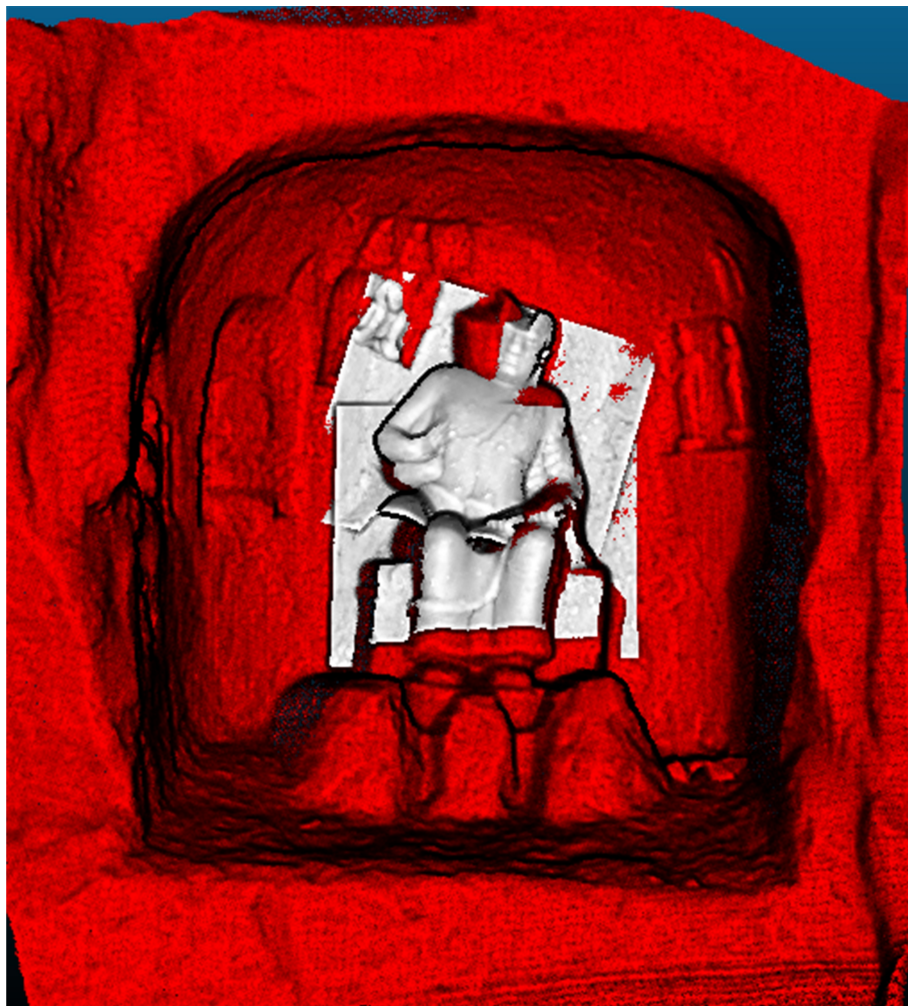
(1)

(2)

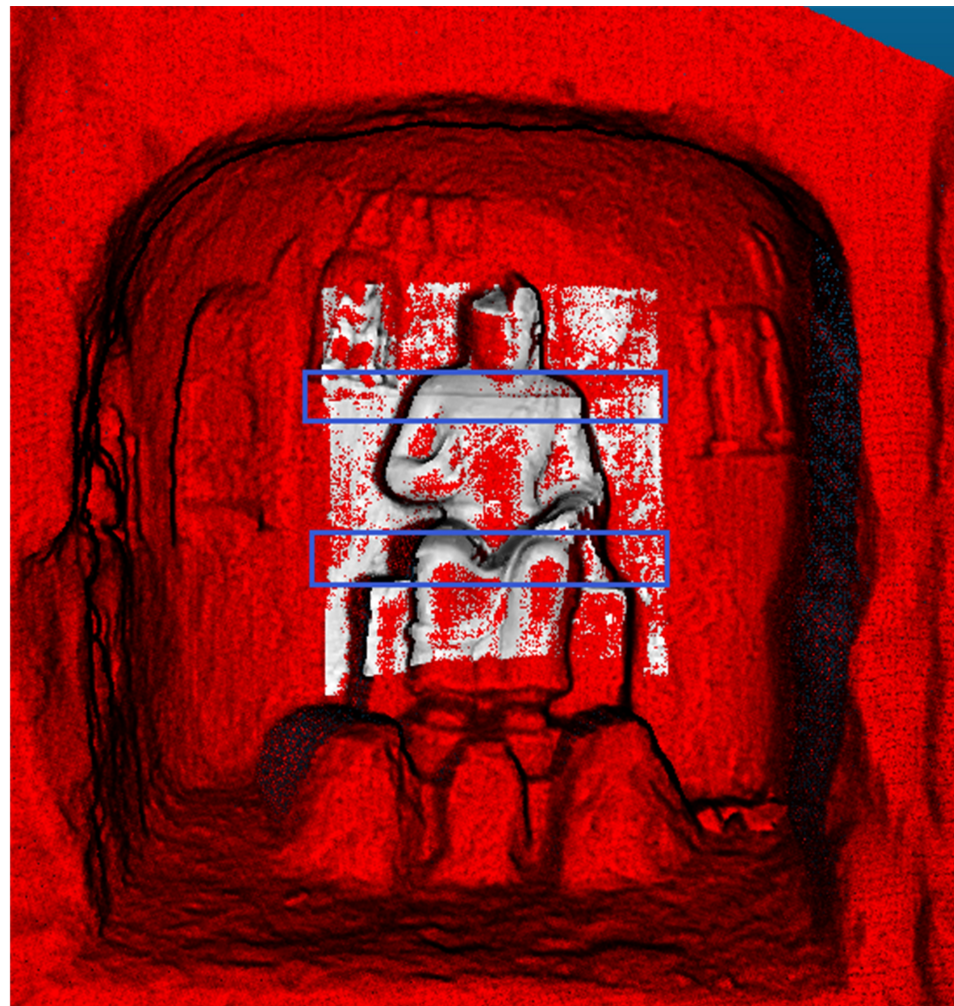
(3)

(4)

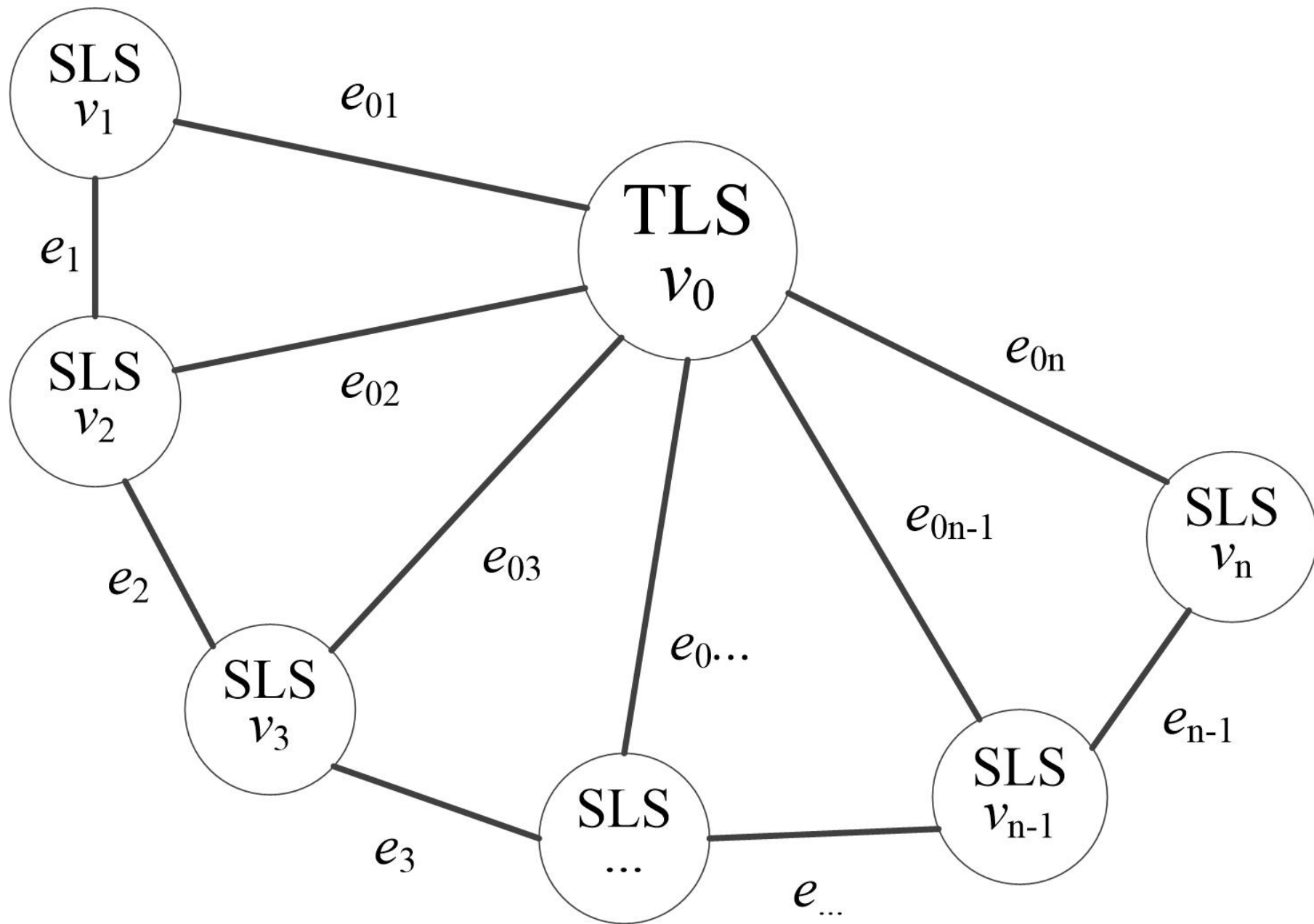
(b)

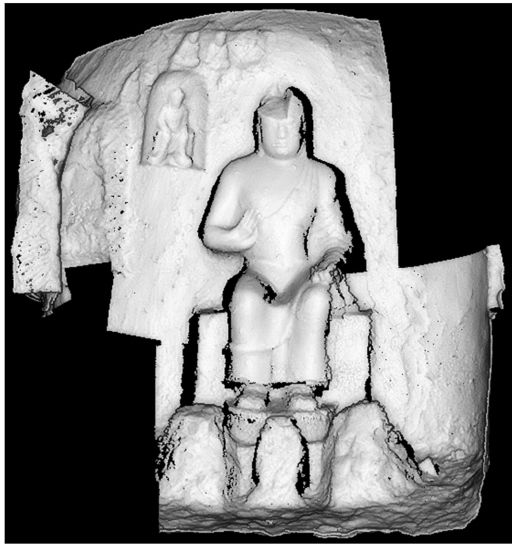


(a)

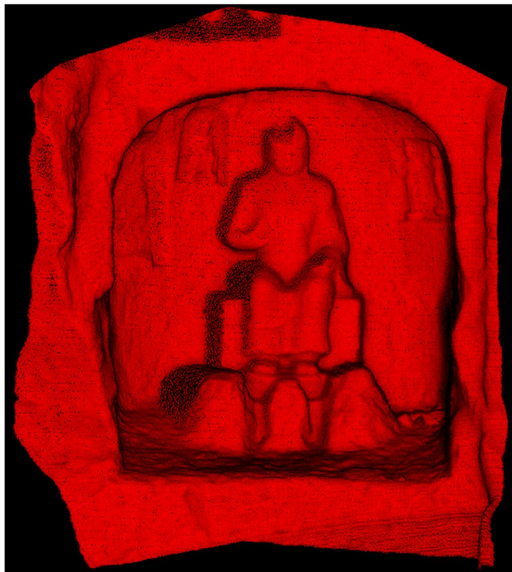


(b)





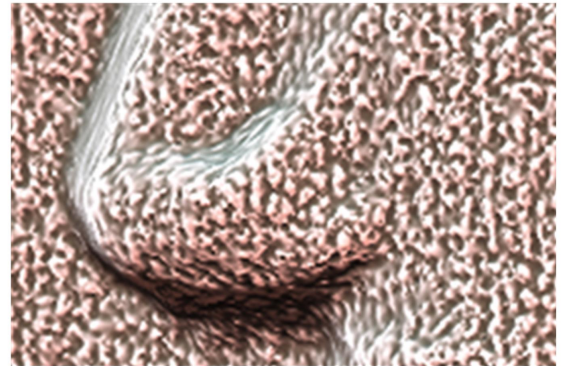
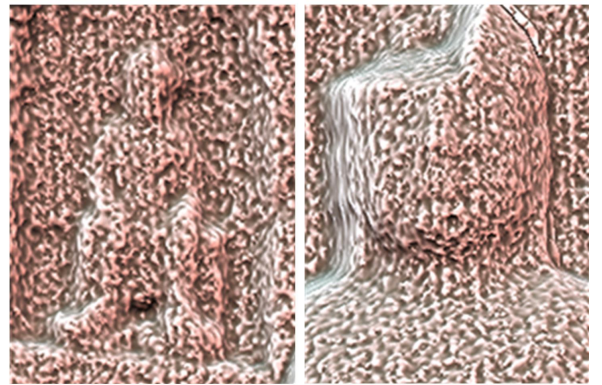
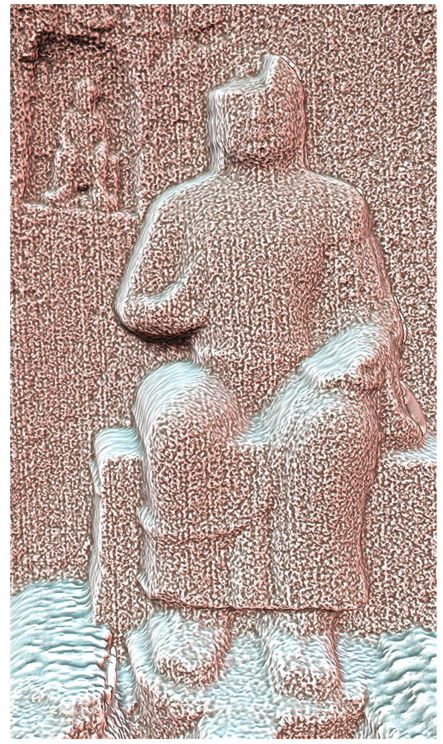
(a)



(b)

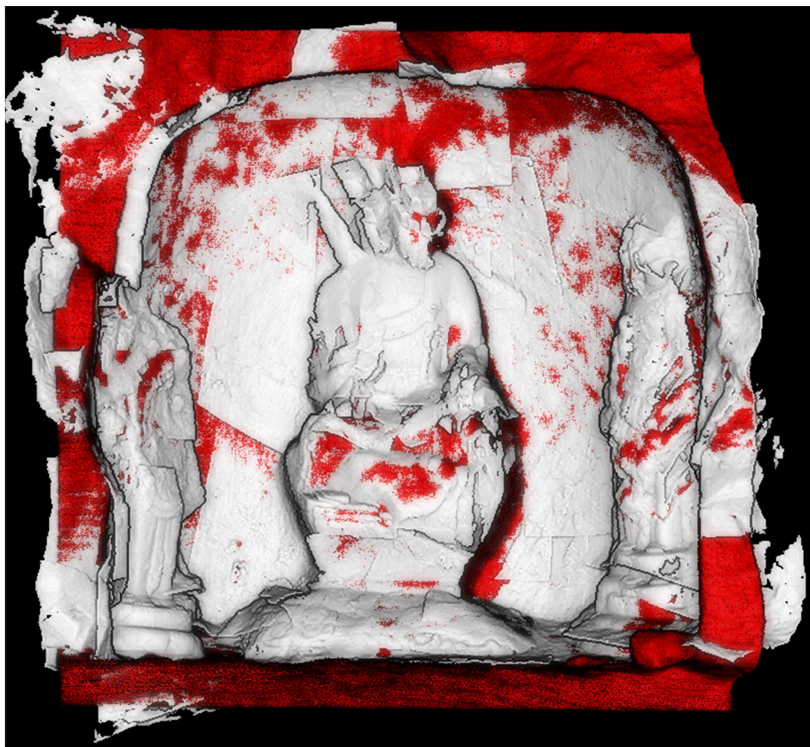


(c)

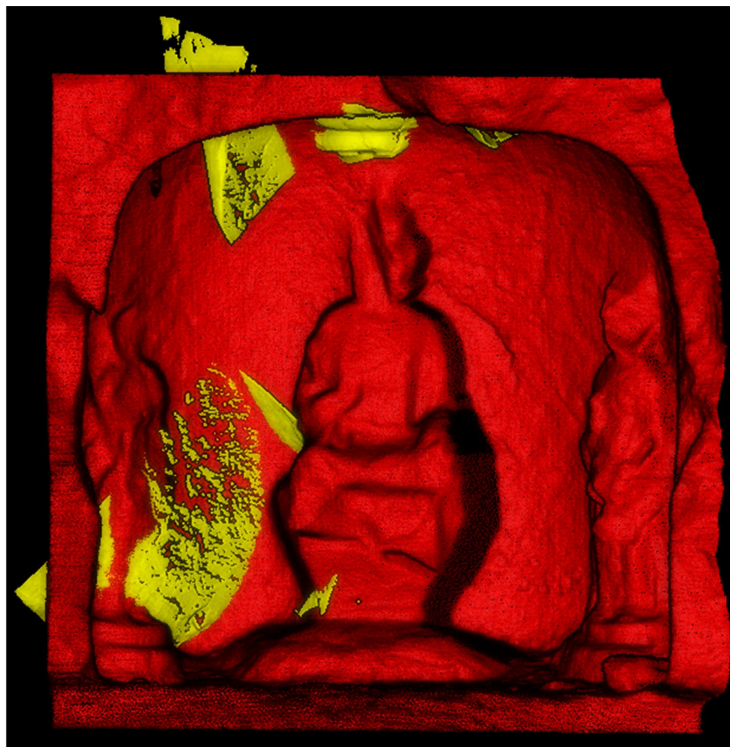


(a)

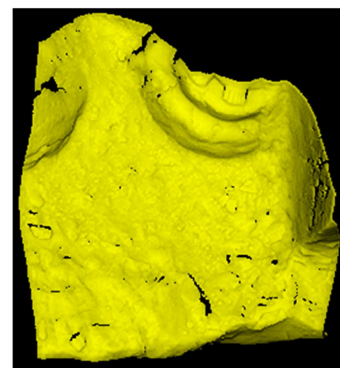
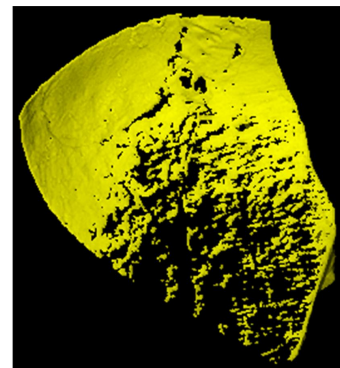
(b)



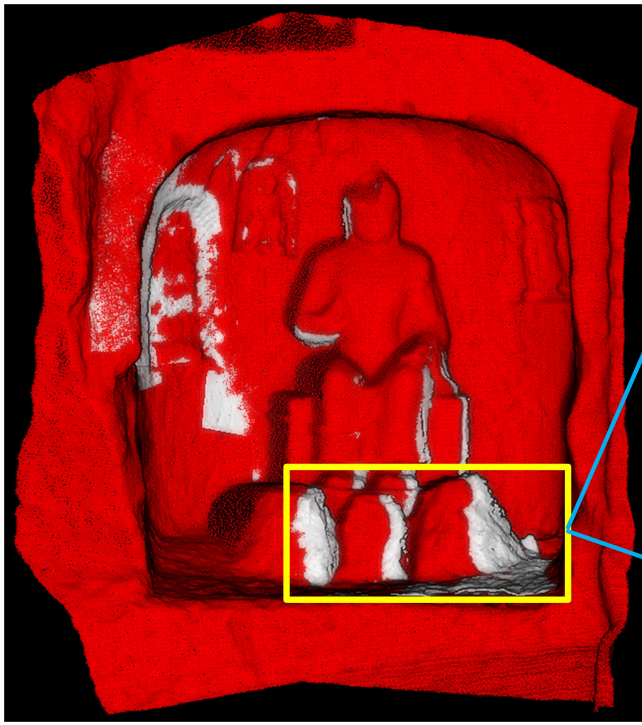
(a)



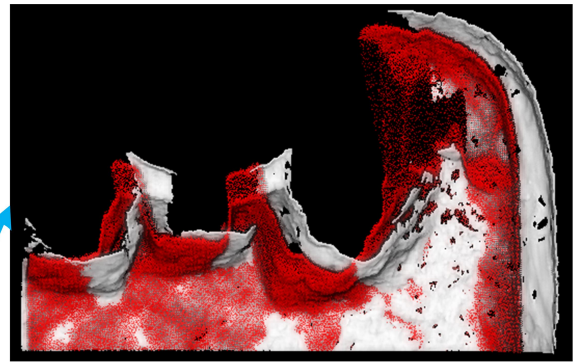
(b)



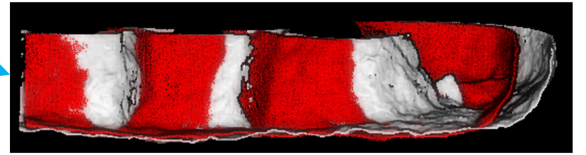
(c)



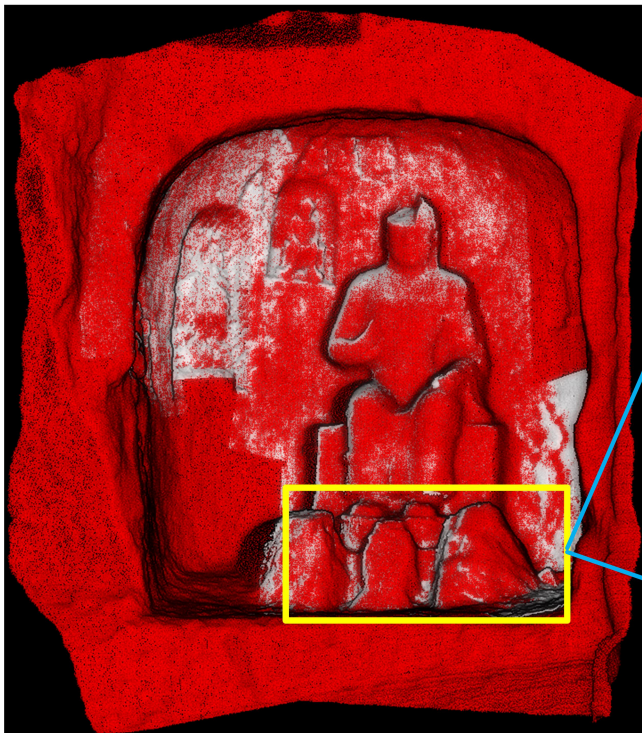
(a)



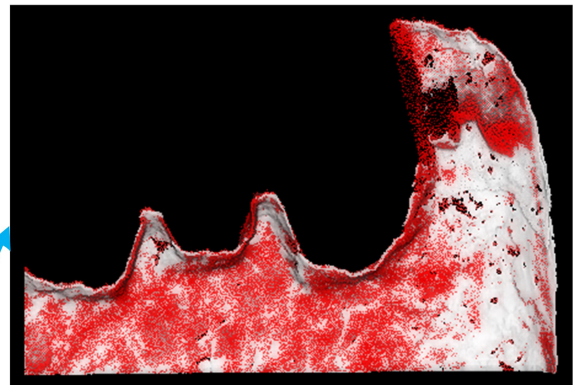
(a-1)



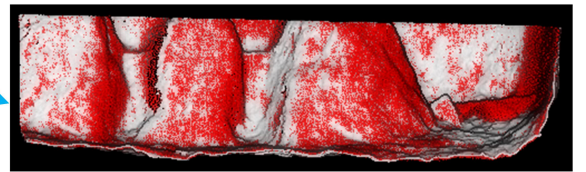
(a-2)



(b)



(b-1)



(b-2)